Science of the Total Environment 755 (2021) 142666

Contents lists available at ScienceDirect

Science of the Total Environment

journal homepage: www.elsevier.com/locate/scitotenv

Methylmercury formation in boreal wetlands in relation to chemical speciation of mercury(II) and concentration of low molecular mass thiols

Van Liem-Nguyen [a,b], Ulf Skyllberg [c], Erik Björn [a,*]

[a] Department of Chemistry, Umeå University, SE-901 87 Umeå, Sweden
[b] Laboratory of Advanced Materials Chemistry, Advanced Institute of Materials Science, Ton Duc Thang University, Ho Chi Minh City, Viet Nam
[c] Department of Forest Ecology and Management, Swedish University of Agricultural Sciences, SE-901 83 Umeå, Sweden

HIGHLIGHTS

- In-depth description of the chemical speciation of Hg in boreal wetlands
- Mercury solid/adsorbed phases identified as a principal factor for Hg methylation
- Mercury methylation correlates with specific low molecular mass thiols.

GRAPHICAL ABSTRACT

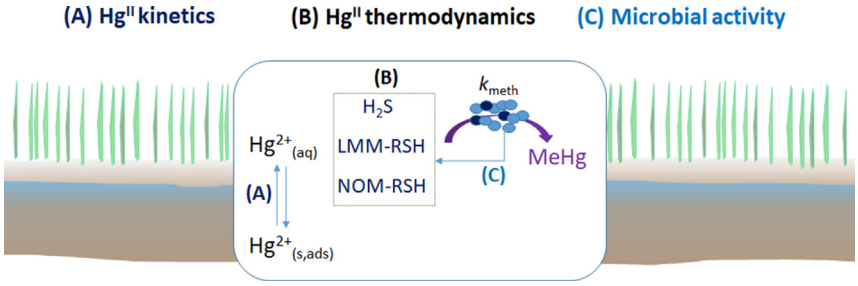

ARTICLE INFO

Article history:
Received 22 June 2020
Received in revised form 22 September 2020
Accepted 22 September 2020
Available online 3 October 2020

Editor: Mae Sexauer Gustin

Keywords:
Mercury methylation
Soil
Bioavailability
Thermodynamics
Kinetics

ABSTRACT

Methylmercury (MeHg) is a neurotoxin formed from inorganic divalent mercury (Hg^{II}) via microbial methylation, and boreal wetlands have been identified as major sources of MeHg. There is however a lack of studies investigating the relationship between the chemical speciation of Hg^{II} and MeHg formation in such environments, in particular regarding to role of thiol compounds. We determined Hg^{II} methylation potentials, k_{meth}, in boreal wetland soils using two Hg^{II} isotope tracers: $^{198}Hg(OH)_2(aq)$ and Hg^{II} bonded to thiol groups in natural organic matter, $^{200}Hg^{II}$–NOM(ads), representing Hg^{II} sources with high and low availability for methylation. The $^{198}Hg(OH)_2(aq)$ tracer was consistently methylated to a 5-fold higher extent than $^{200}Hg^{II}$–NOM(ads), independent of environmental conditions. This suggests that the concentration of Hg^{II} in porewater was a decisive factor for Hg^{II} methylation. A comprehensive thermodynamic speciation model (including Hg^{II} complexes with inorganic sulfide (H_2S), polysulfides (H_2S_n), thiols associated with natural organic matter (NOM–RSH) and specific low molecular mass thiols (LMM–RSH) provided new insights on the speciation of Hg^{II} in boreal wetland porewaters, but did not demonstrate any clear relationship between k_{meth} and the calculated chemical speciation. In contrast, significant positive relationships were observed between k_{meth} and the sum of LMM thiol compounds of biological origin. We suggest two possible mechanisms underlying these correlations: 1) LMM thiols kinetically control the size and composition of the Hg^{II} pool available for microbial uptake, and/or 2) LMM thiols are produced by microbes such that the correlation reflects a relation between microbial activity and MeHg formation.

1. Introduction

The contamination of aquatic and terrestrial ecosystems with methylmercury (MeHg) can constitute a threat to wildlife and human health (Mergler et al., 2007; Scheulhammer et al., 2007). Methylmercury is formed intracellularly through the methylation of inorganic divalent mercury (Hg^{II}) by phylogenically diverse microorganisms (Compeau and Bartha, 1985; Fleming et al., 2006; Gilmour et al., 1992; Hamelin et al., 2011; Kerin et al., 2006) carrying the specific *hgcAB* methylation gene cluster (Gilmour et al., 2013; Parks et al., 2013). The chemical speciation of Hg^{II} in solid/adsorbed (Benoit et al., 2001b; Jonsson et al.,

* Corresponding author.
E-mail address: erik.bjorn@umu.se (E. Björn).

https://doi.org/10.1016/j.scitotenv.2020.142666

2014; Jonsson et al., 2012) and aqueous phases (Adediran et al., 2019; Schaefer and Morel, 2009; Schaefer et al., 2011) is a key factor for MeHg formation by controlling Hg^{II} solubility/partitioning and availability for cellular uptake, respectively. The activity of methylating microbes is predominantly controlled by the availability of metabolic electron donors (Bravo et al., 2017; Drott et al., 2007; Kim et al., 2011) and acceptors (Benoit et al., 2003). The role of the chemical speciation of Hg^{II}(aq) for MeHg formation has been extensively studied in laboratory experiments on model systems (e.g. (Adediran et al., 2019; Benoit et al., 2001a; Schaefer and Morel, 2009; Schaefer et al., 2011)), but there are noteworthy few studies investigating this relation in natural environments (Benoit et al., 1999; Drott et al., 2007; Hollweg et al., 2010).

The chemical speciation of Hg^{II} in oxygen-deficient environments promoting MeHg formation is predominantly controlled by a distribution between complexes with inorganic sulfide (H_2S) and polysulfides (H_2S_n) and organic thiols (RSH) (Skyllberg, 2008). Here we use the term low molecular mass thiols (LMM–RSH) for a specific set of thiol compounds with a molecular mass up to the mass of glutathione (GSH), i.e. 307 Da. The term natural organic matter associated thiols (NOM–RSH) is used for thiol functional groups in natural organic matter molecules where the molecular structure and mass are not identified. The term RSH is used for thiol molecules in general. Appreciable rates of microbial uptake and methylation have been demonstrated in assays with bacteria cultures exposed to Hg^{II} complexes with inorganic sulfide (Benoit et al., 2001b), while lower rates were reported when Hg^{II} complexes with polysulfides dominate (Jay et al., 2002; Kampalath et al., 2013). It has further been demonstrated that the addition of certain LMM–RSH(aq) compounds significantly enhanced cellular uptake and methylation of Hg^{II} in the iron reducing bacterium *Geobacter sulfurreducens*, whereas other LMM–RSH(aq) compounds did not (Schaefer et al., 2011). For the sulfate reducing bacterium *Desulfovibrio desulfuricans* ND132, methylation rates were generally higher and less dependent on the type of LMM–RSH(aq) compound added compared to *Geobacter sulfurreducens*. The mechanisms for how LMM–RSH(aq) compounds influence Hg^{II} methylation are however, not fully clear. It was recently demonstrated that the thermodynamic stability of Hg^{II} complexes is a principal factor controlling Hg^{II} availability for methylation and that less stable complexes with mixed ligation involving LMM–RSH, OH^-, and Cl^- are methylated at higher rates than the more stable $Hg(LMM–RS)_2$ complexes (Adediran et al., 2019). It was further demonstrated that the presence of LMM–RSH compounds (i.e. cysteine) can cause enhanced Hg^{II} methylation by additional mechanisms other than by controlling the speciation of dissolved Hg^{II} (Adediran et al., 2019). The potential relations between LMM–RSH(aq) compounds and MeHg formation in nature also remains elusive (Bouchet et al., 2018; Leclerc et al., 2015). Work including Hg^{II}(aq) complexes formed with specific LMM–RSH(aq) compounds is needed to link the chemical speciation of Hg^{II}(aq) to MeHg formation in natural environments (Benoit et al., 1999; Drott et al., 2007; Hollweg et al., 2010).

In the study presented here, we address three central but understudied aspects of MeHg formation in boreal wetland soils by investigating: (1) if solubility/desorption rate of Hg^{II} is a principal factor controlling the Hg^{II} methylation potential across a wide range of geochemical conditions; (2) if the Hg^{II} methylation potential can be quantitatively predicted by the thermodynamic speciation of dissolved Hg^{II} determined by state-of-the-art models; (3) if MeHg formation is directly or indirectly linked to the concentration of specific LMM–RSH (aq) compounds.

2. Materials and methods

2.1. Sites description and sampling

A detailed description of the boreal wetlands included in this study has been presented previously (Liem-Nguyen et al., 2017a; Tjerngren et al., 2012a; Tjerngren et al., 2012b). In summary, two sites in northern Sweden: Storkälsmyran (SKM) and Kroksjön (KSN) and two sites in southern Sweden: Långedalen (LDN) and Gästern (GTN) were selected to cover boreal wetlands with different soil acidity, nutrient status, Hg^{II} methylation potential and MeHg concentration. The northern wetlands SKM and KSN are of a poor fen type, the latter with some open water, while the southern ones are characterized as a bog-fen gradient at LDN and a mesotrophic wetland-lake at GTN. The sampling procedures were described in detail by Liem-Nguyen et al. (2017a). Briefly, at each of the four sites soil and porewater were sampled at four or five locations with four or five sampling depths at each location generating a total of 77 samples. Wetland porewaters were sampled using a perforated Teflon probe which was inserted into the soil at defined depths and connected to a vacuum pump. A flow of N_2 gas (1 L min^{-1}) was flushed through the sampling system prior to and during porewater sampling to eliminate air from the system. Porewater samples were collected without exposure to ambient air in 250 mL high density polyethylene (HDPE) vessels at 5 cm depth intervals beginning at the water table surface (0 cm level) down to 25 cm. Soil cores corresponding to each 5 cm depth were cut out with a knife and put into double plastic zip-bags after pressing out excess air by hand. All parameters determined in the soil samples thus corresponds to 5 cm depth-integrated conditions. Porewater and soil samples were transported on ice and further handled in a glove box filled with N_2 within a few hours after sampling.

2.2. Determination of the Hg^{II} methylation potential

The Hg^{II} methylation potential (k_{meth}, d^{-1}) was determined using two different enriched Hg isotope tracers, referred to as $^{198}Hg^{II}$(aq) and $^{200}Hg^{II}$–NOM(ads). The $^{198}Hg^{II}$(aq) tracer was prepared by dissolving ^{198}HgO(s) in 14 M HNO_3 followed by dilution with MQ water. The dominant chemical form of Hg^{II} is expected to be $Hg(OH)_2$(aq) in the $^{198}Hg^{II}$(aq) tracer. The $^{200}Hg^{II}$–NOM(ads) tracer was synthesized by mixing 0.55 μmol of $^{200}Hg^{II}$(aq) with 175 mg of an organic peat soil (Skyllberg and Drott, 2010) for 6 h in 30 mL deoxygenated MQ water (end-over-end rotation at 15 rpm). The slurry mixture was then equilibrated in darkness at 4 °C for 5 days (Jonsson et al., 2012). The organic soil was previously sampled at 10–20 cm depth, 10 cm above the groundwater table in a 50 ha forested catchment in northern Sweden (research station Svartberget, 64° 14′ N, 19° 46′ E). The soil was freeze-dried, and Hg and S speciation was characterized by extended X-ray absorption fine structure (EXAFS) spectroscopy and X-ray absorption near edge structure (XANES) spectroscopy (Qian et al., 2002). The molar ratio of total RSH to Hg^{II} is estimated to be on the order of 15 which ensures the formation of $Hg(NOM–RS)_2$ complexes (Liem-Nguyen et al., 2017a). The Hg^{II} isotopes were supplied by the United States Department of Energy Office of Science by the Isotope Program in the Office of Nuclear Physics. For the incubation experiments approximately 10 g of fresh soil was weighed (with two decimals certainty) into two separate 50 mL Falcon (polypropylene, Sarstedt) tubes in the glovebox. To the soil was added 200 μl 0.86 nmol g^{-1} of $^{198}Hg^{II}$(aq) and 200 μl 4.3 nmol g^{-1} of $^{200}Hg^{II}$–NOM(ads) tracers and 1 mL of filtered (0.22 μm PES filter) porewater. One sample set, designated t_0, was immediately frozen (−20 °C) and the other sample set, designated t_{48}, was incubated at room temperature in the glovebox in darkness for 48 h. The relatively long incubation time was chosen because of an expected low k_{meth} of the $^{200}Hg^{II}$–NOM(ads) tracer. The incubation was terminated by freezing the t_{48} sample at −20 °C.

2.3. Chemical analyses

The analyses of relevant ancillary chemical parameters were conducted in situ, or samples were analyzed or preserved in a mobile laboratory associated directly to the field site. The H_2S(aq) concentration and pH in porewaters were measured in situ in the field by inserting perforated alumina porewater tubes to defined depths in the wetland

soils and using a Unisense H_2S NP sensor electrode and Mettler Toledo pH meter InLab Routine Pro electrode, respectively. Collected samples were filtrated through a 0.22 μm funnel filter using a vacuum pump in the glove box. Total Hg in filtered porewaters was determined by isotope dilution analysis (IDA) using a mercury cold vapor generation system hyphenated to inductively coupled plasma mass spectrometry (ICPMS) (USEPA, 2002). The concentration of MeHg was determined by IDA using direct ethylation with sodium tetraethylborate (STEB) and purge and trap onto a Tenax adsorbent and subsequent analysis by thermal desorption gas chromatography ICPMS (TDGC-ICPMS) (Lambertsson and Bjorn, 2004). The concentration of Hg^{II} was calculated by subtracting the MeHg concentration from the total Hg concentration. Concentrations of LMM–RSH(aq) compounds and the corresponding organic disulfide forms, RSSR(aq), were determined by liquid chromatography electrospray ionization mass spectrometry (LC-ESIMS) (Liem-Nguyen et al., 2015). The concentration of thiol groups associated with NOM (NOM–RSH) was determined by a combined approach using Hg L_{III}-edge EXAFS spectroscopy and S K-edge XANES spectroscopy (beamline I811 at MAX-II, Lund, Sweden) (Liem-Nguyen et al., 2017a). In summary, the RSH(aq) concentration was determined by Hg L_{III}-edge EXAFS for selected pooled samples taken at sites GTN and LDN. Based on these two samples RSH was estimated to be 15% of the total organic reduced sulfur content ($OrgS_{RED}$), as determined by S K-edge XANES. This number was thereafter fixed for the larger set of samples for which S XANES determinations were conducted. For soil samples, total Hg was determined by solid combustion atomic absorption spectrometry (AMA 254, Leco), and total MeHg was determined by GC-ICPMS after solvent double extraction and STEB derivatization (Lambertsson et al., 2001). The concentration of Hg^{II} was calculated by subtracting the MeHg concentration from the total Hg concentration. Elemental sulfur (S^0) in soil was extracted and measured by reversed phase liquid chromatography with UV absorption detection (Burton et al., 2011). The determination of additional ancillary chemistry parameters, and quality control measures for the Hg and thiol analyses, are described in the supporting information (SI text 1).

2.4. Chemical speciation modeling

The chemical speciation of Hg^{II} in wetland soils and porewaters was modeled using the WinSGW software from Majo, Umeå, Sweden (Karlsson and Lindgren, 2012). The model comprised 15 components and 77 species, including Hg^{II} complexes with inorganic sulfides (H_2S(aq)), polysulfides (H_2S_n(aq)), thiols associated with natural organic matter (NOM–RSH(aq)) and specific LMM–RSH(aq) ligands detected in the wetland porewaters (Table S1). The model was adapted from Liem-Nguyen et al. (2017a) but refined to also include individual specific $Hg(LMM–RS)_2$(aq), Hg(LMM–RS)(aq) and Hg(LMM–RS)(NOM–RS)(aq) complexes using recently established stability constants (Liem-Nguyen et al., 2017b). The reactions (1) to (10) are thus the most influential ones, controlling the chemical speciation of Hg^{II} in the wetland soils (Eq. (1) Schwarzenbach, 1963; Eq. (2) Dyrssen and Wedborg, 1991; Eq. (3) Jay et al., 2000; Eq. (4) Drott et al., 2013; Liem-Nguyen et al., 2017a; Schwarzenbach, 1963; Eq. (5) Liem-Nguyen et al., 2017a; Liem-Nguyen et al., 2017b; Eq. (6) Liem-Nguyen et al., 2017a; Skyllberg, 2008; Eq. (7) Liem-Nguyen et al., 2017b; Song et al., 2018; Eq. (8) Millero, 1986; Eq. (9) Liem-Nguyen et al., 2017b; Eq. (10) Liem-Nguyen et al., 2017a; Skyllberg, 2008).

$$Hg^{2+} + 2HS^- = Hg(SH)_2{}^0(aq);\ \log K = 38.6 \quad (1)$$

$$Hg^{2+} + 2HS^- = HgS_2H^-(aq) + H^+;\ \log K = 32.2 \quad (2)$$

$$Hg^{2+} + 2HS^- + (n-1)S_{orth}{}^0 = HgS_nSH^-(aq) + H^+;\ \log K = 32.6 \quad (3)$$

$$Hg^{2+} + HS^- = HgS(s) + H^+;\ \log K = 37.3 \quad (4)$$

$$Hg^{2+} + 2LMM–RS^- = Hg(LMM–RS)_2;\ \log K = 37.5–41.5 \quad (5)$$

$$Hg^{2+} + 2NOM–RS^- = Hg(NOM–RS)_2;\ \log K = 41.0 \quad (6)$$

$$Hg^{2+} + LMM–RS^- + NOM–RS^- = Hg(LMM–RS)(NOM–RS);\ \log K = 39.3–41.3 \quad (7)$$

$$H_2S(aq) = HS^- + H^+;\ \log K = 7.0 \quad (8)$$

$$LMM–RS^- + H^+ = LMM–RSH;\ \log K = 7.34–10.33 \quad (9)$$

$$NOM–RS^- + H^+ = NOM–RSH;\ \log K = 9.0 \quad (10)$$

The ranges given for log *K* values of reactions (5), (7) and (9) represent the intervals for the LMM-RSH compounds cysteine (Cys), mercaptoacetic acid (MAC), 2-mercaptopropionic acid (2-MPA), monothioglycerol (Glyc), homocysteine (HCys), *N*-acetylcysteine (NACCys), and glutathione (GSH). Values of the stability constants selected for reactions (1), (4), (6) and (10) were based on optimized model fits to wetland porewater data on aqueous Hg^{II} concentrations reported by Liem-Nguyen et al. (2017a) and Song et al. (2018) recently published refined log *K* values for the above reaction (6) and for reaction (7) with Cys as the LMM–RSH compound. Together the data from Liem-Nguyen et al. (2017b) and Song et al. (2018) on Hg^{II} complexes with RSH compounds form an internally consistent thermodynamic database, which we propose is used to model the chemical speciation of Hg^{II} in systems with LMM and NOM associated thiols. These constants have however not yet been evaluated against constants for Hg^{II} complexes with sulfide and in this study we have therefore kept the log *K* of 41.0 for reaction (6) from Liem-Nguyen et al. (2017a). The derivation of log *K* values for reaction (7) is discussed further in SI text 2. As discussed by Liem-Nguyen et al. (2017a) competition from borderline/soft trace metals is not expected to affect the chemical speciation of Hg^{II} in these soils.

3. Results and discussion

3.1. Biogeochemical characteristics of the boreal wetland sites

To address our study objectives, we designed a sampling campaign to obtain significant gradients in: i) porewater concentrations of DOC, Fe, H_2S, Hg and MeHg, ii) the chemical speciation of Hg^{II}, and iii) the magnitude of the Hg^{II} methylation potential (k_{meth}). The key biogeochemical parameters determined in wetland porewater and soil are summarized in Table 1. Part of this data is reproduced from Liem-Nguyen et al. (2017a) as specified in Tables S2 and S3. Additional descriptive parameters of these sites have been presented in previous studies (Tjerngren et al., 2012a; Tjerngren et al., 2012b). The numerical values for most of the parameters in Table 1 span about two orders of magnitude, and the concentrations of H_2S(aq) and Fe^{II}(aq) span three orders of magnitude. The study sites thus represent broad ranges in relevant geochemical conditions encountered in boreal wetlands. The sites were characterized by a relatively low pH (4.16–6.16) and high content of soil organic matter (9.3–52% of the dry mass) and porewater DOC (18–440 mg L^{-1}). On average, the soil organic matter content and DOC concentration were 39% of dry mass and 71 mg L^{-1}, respectively but considerably lower only at site KSN. The redox conditions ranged from ferruginous (maximum 370 μM Fe^{II}(aq) and < 0.15 μM H_2S(aq)) to sulfidic (maximum 270 μM H_2S(aq)). We did not detect any mackinawite type FeS(s) phases, as judged by S XANES spectroscopy measurements of soil samples. Based on concentrations of Fe(II) and sulfide and well-established thermodynamic constants, FeS(s) was not thermodynamically stable in the soils, with the possible exception of three soil samples from the GTN site having sulfide concentrations exceeding 180 μM (Tables S2a and S5) (Liem-Nguyen et al., 2017a). Total concentrations of NOM-RSH(aq) in porewater samples ranged

Table 1
Concentration ranges of key geochemical parameters in boreal wetland (a) porewaters and (b) soils.

(a)

Porewater

	pH	Hg(II)	MeHg	H_2S(aq)[a]	Σ LMM-RSH(aq)	Σ LMM-RSH + RSSR(aq)	RSH(aq)	Cl^-	Fe(II)	DOC	Ionic strength
		pM	pM	μM	nM	nM	μM	mM	μM	mg L^{-1}	M
Min	4.16	2.17	0.65	<0.15[a]	<0.10	2.5	0.32	0.01	0.05	18	0.0004
Max	6.16	560	92	270	77	130	23	0.42	370	440	0.005
Average	5.10	87	9.4	16	14	33	2.9	0.16	39	71	0.002

(b)

Soil (dry mass)

	Hg^{II}(ads)	MeHg(ads)	RSH(ads)	S^0	Total C	Total N	Dry mass
	pmol g^{-1}	pmol g^{-1}	μmol g^{-1}	μmol g^{-1}	%	%	%
Min	89	1.9	2.8	0.01	9.3	0.60	2.7
Max	1500	160	22	4.0	52	2.5	61
Average	590	39	10	0.60	39	1.6	15

[a] The minimum H_2S(aq) concentration of 0.15 μM corresponds to half the detection limit value of 0.3 μM of the H_2S NP sensor electrode used.

from 0.32 μM to 23 μM with an average of 2.9 μM, as determined by combined Hg L_{III}-edge EXAFS and S K-edge XANES spectroscopy measurements (Liem-Nguyen et al., 2017a). Ten specific LMM-RSH(aq) compounds were detected in the wetland porewaters by LC-ESIMS (Liem-Nguyen et al., 2015): cysteine (Cys), N-acetyl−cysteine (NACCys), glutathione (GSH), penicillamine (Pen), homocysteine (HCys), γ-glutamylcysteine (GluCys), mercaptoacetic acid (MAC), monothioglycerol (Glyc), 2-propionic acid (2MPA) and mercaptosuccinic acid (SUC). The compounds Cys, NACCys, and MAC were the most frequently detected. The concentration of each detected LMM-RSH(aq) compound varied from sub nM to 24 nM except for Glyc which reached a concentration of up to 77 nM in KSN porewater samples, but was not detected at the other sites. The sum of these ten specific LMM-RSH(aq) compounds constituted a minor fraction (average 0.28%) of the total NOM-RSH(aq) concentration in porewater. Most previous studies on LMM thiols in natural waters have reported the total concentration of the thiol (RSH) and disulfide (RSSR) forms for each compound. We determined the concentration of both the thiol form and the sum of RSH(aq) + RSSR(aq) for each LMM-RSH(aq) compound (Tables 1, S4a, b). This distinction is important as Hg^{II} forms strong complexes with RSH, but not with RSSR compounds and in the chemical speciation model we therefore used the concentration of RSH(aq) compounds only. Depending on the redox condition in the sample, the RSH (aq) form constituted 5–90% (with an average of 40%) of the sum RSH (aq) + RSSR(aq) for the LMM thiols detected in these wetland samples.

3.2. Time dependent solubility of Hg^{II} as related to MeHg formation

We determined the Hg^{II} methylation potential (k_{meth}) in soil incubation experiments using two different enriched Hg^{II} isotope tracers. One tracer, $^{198}Hg^{II}$(aq), was added to soil incubations as a labile dissolved complex, $^{198}Hg(OH)_2$(aq), and the other tracer, $^{200}Hg^{II}$–NOM(ads), was added as a $^{200}Hg(NOM\text{-}RS)_2$(ads) structure, as verified by Hg EXAFS (Skyllberg et al., 2006). The purpose of the dual-tracer approach was to evaluate quantitative differences in k_{meth} for an equilibrated tracer with comparably low availability (the $^{200}Hg^{II}$–NOM(ads) tracer), and a tracer representing a Hg substrate of maximum availability (the $^{198}Hg^{II}$(aq) tracer) for methylation. Fig. 1 demonstrates a significant positive correlation ($r2 = 0.88$, $p < 0.001$) between k_{meth} determined with the two tracers. Notably the k_{meth} was a factor of 5 higher for $^{198}Hg^{II}$(aq) than for $^{200}Hg^{II}$-NOM(ads) throughout the data set. This means that independent of geochemical factors like pH, DOC and H_2S, the $^{198}Hg^{II}$(aq) tracer was always about a factor of 5 more available for methylation than the $^{200}Hg^{II}$–NOM(ads) tracer. The two tracers are expected to show very different time-dependent concentrations of total Hg^{II} in porewater. The $^{198}Hg(OH)_2$(aq) tracer is expected to be very reactive and rapidly change its speciation by exchange reactions with dissolved LMM–RSH, H_2S and NOM–RSH(aq) ligands whereas reactions with reactive soil surfaces, such as NOM–RSH(ads), are expected to be somewhat slower. Also steric hindrance and other "aging effects" of newly formed solid and surface Hg^{II} phases will only gradually slow down the bioavailability of the $^{198}Hg(OH)_2$(aq) tracer. The total porewater Hg^{II} concentration is therefore expected to decrease with time, at least initially, during the 48 h of our incubations. Olsen et al. (2018) recently presented a refined kinetic model for k_{meth} determinations, taking into account sorption reactions leading to decreased availability for methylation over time of an added labile dissolved complex ($HgCl_2$ in their study). In contrast, the added $^{200}Hg(NOM\text{-}RS)_2$(ads) complex is thermodynamically very stable and its structure likely sterically hindered (Jiskra et al., 2014). As a consequence, the $^{200}Hg^{II}$–NOM (ads) tracer is expected to react slower with dissolved ligands and the Hg^{II} porewater concentration, as represented by aqueous complexes with LMM-RSH, H_2S and NOM-RSH(aq), will initially be low and increase with time. Thus, the result demonstrating a 5-fold higher

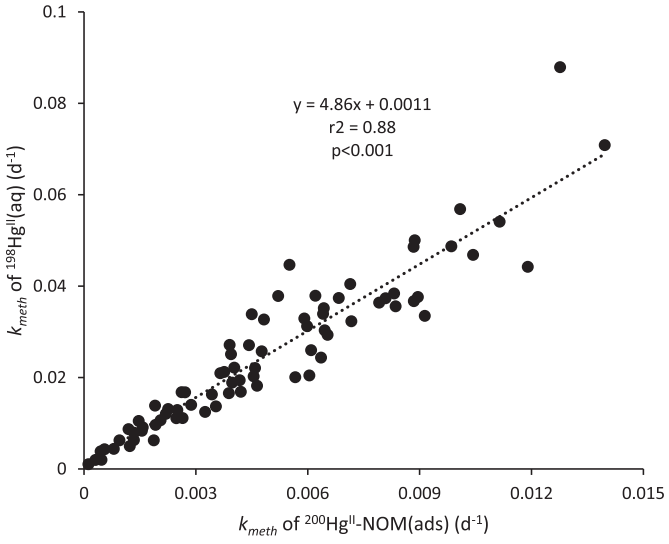

Fig. 1. Correlation between the Hg methylation rate constant (k_{meth}, d^{-1}) determined by a dissolved labile $^{198}Hg^{II}$(aq) tracer and an adsorbed phase $^{200}Hg^{II}$-NOM(ads) tracer.

methylation potential of the $^{198}Hg(OH)_2(aq)$ tracer in Fig. 1 suggests that the chemical speciation of Hg^{II} in solid/adsorbed phases is one decisive factor controlling MeHg formation in boreal wetland soils, independent of geochemical status. The mechanistic interpretation is that the chemical speciation of Hg^{II}(s,ads) causes kinetic constraints of the total Hg^{II} concentration in porewater thereby limiting the pool of Hg^{II} available to form complexes which can pass the cell membranes of methylating microbes (Jonsson et al., 2012; Zhu et al., 2018). Previous studies have demonstrated similar differences in methylation for Hg^{II} tracers with different solubility and/or desorption kinetics in estuarine sediment from single sites (Jonsson et al., 2014; Jonsson et al., 2012; Liem-Nguyen et al., 2016). Our study demonstrated that the difference in methylation potential remained consistent throughout wetland soils with highly contrasting geochemical properties that corroborated Hg^{II} solubility and sorption-desorption as one primary controlling factor for MeHg formation in nature. The results however also show that the methylation of both Hg^{II} tracers in addition is driven by some other common factor (discussed further below) as the k_{meth} for both tracers span two orders of magnitude across the entire data set.

3.3. Chemical speciation of $Hg^{II}(aq)$ in porewater as related to MeHg formation

Results from bacteria culture experiments show that rates of cellular uptake and methylation of $Hg^{II}(aq)$ is not only dependent on the total concentration of dissolved Hg^{II}, but differ substantially depending on ligand composition in the medium (Adediran et al., 2019; Chiasson-Gould et al., 2014; Jay et al., 2002; Schaefer and Morel, 2009; Schaefer et al., 2011). The highest rates have been ascribed to $HgOH_nCl_{2-n}$ complexes and then in decreasing order ternary complexes involving LMM-RSH, OH^- and Cl^- (i.e. $HgOH_nCl_{1-n}$(LMM-RS)), specific $Hg(LMM\text{-}RS)_2(aq)$ complexes (in particular $Hg(Cys)_2$), $Hg(SH)_2^0(aq)$ and the lowest rates to $Hg^{II}(aq)$ complexes with polysulfides and "bulk" dissolved NOM(aq). It is however uncertain to what extent MeHg formation can be predicted by the chemical speciation of dissolved Hg^{II} in natural environments. We developed and applied a refined state-of-the art thermodynamic model for the chemical speciation of $Hg^{II}(aq)$ and Hg^{II}(s,ads) in the wetlands studied here. Calculated average concentrations of $Hg(SH)_2^0(aq) + HgS_2H^-(aq)$, $HgS_nSH^-(aq)$, $\sum Hg(NOM\text{-}RS)_2(aq)$, $\sum Hg(NOM\text{-}RS)(LMM\text{-}RS)(aq)$ and $\sum Hg(LMM\text{-}RS)_2(aq)$ in the porewaters were 26 ± 30 pM, 32 ± 57 pM, 29 ± 78 pM, 0.013 ± 0.039 pM and 0.000011 ± 0.000038 pM, respectively. Fig. 2 illustrates how the concentration of these $Hg^{II}(aq)$ complexes, and the solid HgS (s) and adsorbed $Hg(NOM\text{-}RS)_2(ads)$ phases, varied across all wetland samples. Figs. S1 and S2 show the concentrations of reduced sulfur ligands in the samples and the concentration ranges of the Hg^{II} complexes. Because of the low pH, $H_2S(aq)$ ($pK_a = 7.0$) was the dominant species of dissolved inorganic sulfide in porewaters and we therefore applied in situ measurement (H_2S sensor electrode) of the $H_2S(aq)$ species to minimize losses and ensure high accuracy. For 35 out of 77 of the porewater samples (Fig. 2) the concentration of $H_2S(aq)$ was below the detection limit (0.3 μM) and the concentration was set to half the detection limit value for these samples. Mercury complexes with Cl^- and OH^- were predicted to be insignificant in the wetland soils.

Although the average concentrations of $Hg^{II}(aq)$ complexes formed with sulfides, polysulfides and thiols were very similar, the data set span a range in chemical speciation of $Hg^{II}(aq)$ from a dominance of Hg^{II}-thiol complexes (samples 1 to 20, Fig. 2) to a dominance of Hg^{II}-sulfide and Hg^{II}-polysulfide complexes (samples 42 to 77, Fig. 2). The 10 detected LMM-RSH(aq) compounds contribute to the $Hg^{II}(aq)$ speciation mainly via ternary complexes of the type Hg(LMM-RS)(NOM-RS)(aq) while the concentrations of $Hg(LMM\text{-}RS)_2(aq)$ complexes were very low. A partial least squares regression (PLS) model was generated to investigate possible quantitative relationships between the concentration of dissolved Hg^{II} species in porewater (X-variables) and k_{meth} (Y-variable), PLS model I (SI text 3). The model included in total 50 Hg^{II} species (Table S1). Despite the large variability in concentration and chemical speciation of $Hg^{II}(aq)$ in the porewater samples, no significant correlation ($R^2 = 0.14$, $Q^2 < 0$) was observed between the $Hg^{II}(aq)$ speciation and k_{meth}, examples are given in Fig. S3. The lack of correlation

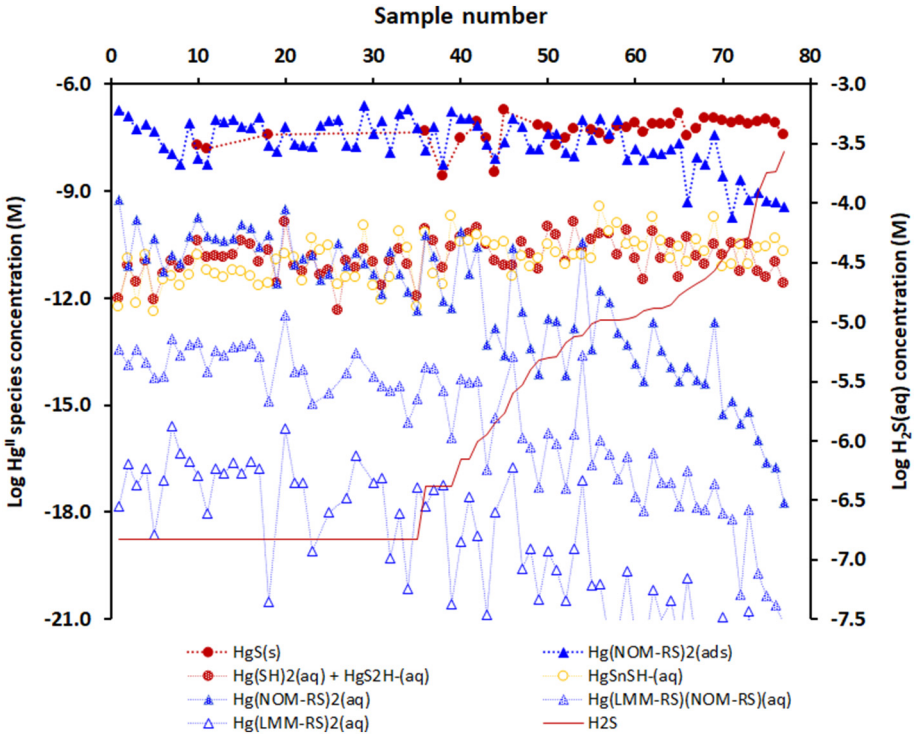

Fig. 2. Concentrations of Hg^{II} species in wetland soil ($HgS(s)$, $Hg(NOM\text{-}RS)_2(ads)$) and porewater ($Hg(SH)_2^0(aq) + HgS_2H^-(aq)$, $HgS_nSH^-(aq)$, $Hg(NOM\text{-}RS)_2(aq)$, $Hg(LMM\text{-}RS)(NOM\text{-}RS)(aq)$, $Hg(LMM\text{-}RS)_2(aq)$) samples, and concentration of $H_2S(aq)$ in porewater. Sample numbers are arranged from low to high concentration of $H_2S(aq)$. Samples with $H_2S(aq)$ concentration below detection limit are arranged from high to low concentration of RSH(aq). The left-hand x-axis is cut at 10^{-21} M.

was observed for both the $^{198}Hg(OH)_2(aq)$ tracer, which is expected to decrease in availability over time during the incubation, and the $^{200}Hg^{II}$–NOM(ads) tracer which is pre-equilibrated with strong binding sites in the adsorbed phase. This shows that the lack of correlation between $Hg^{II}(aq)$ speciation and k_{meth} was not a consequence of a gradual redistribution to stronger binding sites of the labile $^{198}Hg(OH)_2(aq)$ tracer during the incubation experiment (Schwartz et al., 2019).

It should be noted that our results do not contradict the well-established importance of the chemical speciation of dissolved Hg^{II} for bacterial uptake and subsequent methylation, and there are several possible reasons for the observed lack of relation between Hg^{II} speciation and methylation potential in the wetland soils. Differences in availability for methylation among $Hg^{II}(aq)$ species are not taken into account in models where k_{meth} is correlated with only the concentration of Hg^{II} species. This limitation is a possible reason for the lack of correlation obtained with PLS model I and the data in Fig. S3. Species-specific k_{meth} values have been established in laboratory experiments with monocultures for several $Hg(LMM\text{-}RS)_2$ species and for $Hg(SH)_2$ but not for $HgS_nSH^-(aq)$ or $\sum Hg(NOM\text{-}RS)_2(aq)$ species (Adediran et al., 2019; Schaefer et al., 2011). Since the latter two species together constitute on average about 2/3 of the total $Hg^{II}(aq)$ pool in our porewater dataset, it is not feasible to explore if a species-specific k_{meth} rate model could explain observed Hg(II) methylation rates in the studied wetland soils. Further, the molecular structure is unknown for the vast majority of the Hg-thiol complexes present in the wetland soil porewaters. The $Hg(LMM\text{-}RS)_2(aq)$ and Hg(LMM–RS)(NOM–RS)(aq) complexes on average constituted only 0.000037% and 0.046%, respectively of the total $Hg(NOM\text{-}RS)_2(aq)$ pool, Fig. 2. It is thus possible that the expected variability in the molecular composition and availability for methylation of different types of complexes having the local structure of $Hg(NOM\text{-}RS)_2(aq)$, if known, could explain the variability in k_{meth} in the wetland soils. However, it may be just as likely that the expected complex mixture of different types of thiol compounds forms a continuum in availability for methylation of Hg^{II} complexes that do not vary substantially across our dataset, and thus cannot explain the variability in k_{meth}. It is interesting to note that there was no difference in the average k_{meth} of samples in which the chemical speciation of $Hg^{II}(aq)$ was dominated by complexes with either thiols (samples 1–20 in Fig. 2) or by complexes with sulfide and polysulfides (samples 40–77 in Fig. 2). This may suggest that the concentration of ligands forming bioavailable complexes with $Hg^{II}(aq)$ is sufficiently large throughout the data set, such that the formation of specific dissolved $Hg^{II}(aq)$ complexes in the porewater is not rate limiting for MeHg formation in these soils. To resolve the different possibilities here, our results point at the importance of a more detailed characterization of the molecular composition of NOM-RSH(aq) compounds, and that species-specific methylation rate constants of the corresponding Hg^{II} complexes need to be determined to further advance our understanding of Hg^{II} availability for methylation in wetland soils.

3.4. Relationship between LMM thiol compounds and MeHg formation

We generated a second PLS model (PLS model II, SI text 3) with measured k_{meth} as Y-variable and with ancillary chemistry parameters determined in this study as X-variables (69 in total). This model could explain and predict about half ($R^2 = 0.62$, $Q^2 = 0.47$) of the observed variability in k_{meth} in the whole dataset. The two most important parameters correlating with k_{meth} were the RSH + RSSR sum concentrations for the 10 detected LMM thiols and a subset of LMM thiols of direct biological origin (as discussed further below). The significant correlation between RSH + RSSR concentrations of all detected LMM thiols and k_{meth} are illustrated in Fig. S4. This result is in agreement with, and corroborates, two recent studies demonstrating a correlation between the concentration of LMM–RSH compounds and MeHg concentration (Leclerc et al., 2015) or k_{meth} (Bouchet et al., 2018) in aquatic biofilms. Leclerc et al. (2015) reported concentrations up to ~400 nM of the sum of RSH + RSSR forms for a set of LMM thiols in autotrophic biofilms and demonstrated a significant relationship between the concentrations of Cys, GluCys and GSH and MeHg concentration in the colloidal fraction (but not the capsular fraction) of the biofilms. Bouchet et al. (2018) reported concentrations up to ~3500 nM of RSH + RSSR forms of LMM thiols in epibenthic biofilms and *Characeæs*' periphyton, and demonstrated a significant correlation between the sum concentration of LMM thiols and k_{meth}. In both studies, it was proposed that these thiol compounds may affect the availability of Hg^{II} to methylating microbes in the biofilms. This hypothesis was however, not tested because of an (intentional) incomplete characterization of Hg^{II} binding ligands in the systems, and the mechanistic relation underlying the observed correlation between LMM thiols and MeHg formation is not fully clear. Our speciation and methylation rate modeling results (Fig. 2, Figs. S3 and S5, PLS model I) suggest that the correlation between LMM thiols and k_{meth} may be caused by other mechanisms than LMM–RSH compounds controlling the bioavailable pool of thermodynamically stable $Hg^{II}(aq)$ species in porewater. In recent laboratory assay experiments with *Geobacter sulfurreducens* Adediran et al. (2019) demonstrated that addition of 50–500 nM Cys enhanced methylation without causing significant changes in the thermodynamic speciation of $Hg^{II}(aq)$. The speciation was largely dominated by the $Hg(Cys)_2$ complex at all Cys additions. The results from our study and Adediran et al. thus suggest that LMM–RSH compounds can affect Hg^{II} methylation via additional mechanisms than by controlling the thermodynamically predicted speciation of $Hg^{II}(aq)$ in the extracellular medium.

It is possible that LMM–RSH compounds control bioavailability of $Hg^{II}(aq)$ via kinetic constraints on the chemical speciation of $Hg^{II}(aq)$. The chemistry, including the speciation of $Hg^{II}(aq)$, at bacterial surfaces may differ significantly from bulk soil and porewater, for example due to the secretion of LMM thiols and inorganic sulfide by microbes. In the study by Leclerc et al., up to three orders of magnitude higher concentrations of LMM thiols were observed extracellularly in biofilms as compared to the bulk water column in a studied Boreal Shield lake (Leclerc et al., 2015). If ligand exchange rates between different $Hg^{II}(aq)$ complexes with LMM thiols and sulfide are sufficiently fast (Pei et al., 2011; Rabenstein and Isab, 1982), significant changes in the chemical speciation of $Hg^{II}(aq)$, not predicted by thermodynamic models for bulk porewater, may occur at bacteria surfaces prior to cellular uptake. Indeed it has been suggested that interactions between $Hg^{II}(aq)$ and DOM can kinetically constrain the size of the Hg^{II} pool available for methylating microbes (Chiasson-Gould et al., 2014). In addition to the species in Fig. 2, our chemical speciation model also included Hg–LMM thiol species with 1:1 stoichiometry, ternary complexes of the type $HgOH_nCl_{1-n}(LMM\text{–}RS)$ and Hg^{II} complexes with OH^- and Cl^- ligands, Table S1. The study by Adediran et al. (2019) demonstrated higher k_{meth} for thermodynamically less stable complexes of the types $HgOH_nCl_{2-n}(aq)$, $HgOH_nCl_{1-n}(LMM\text{-}RS)(aq)$ and Hg(LMM-RORS)(aq) (Hg^{II} coordinated to one S and one O atom in the same LMM-RSH molecule) compared to $Hg(LMM\text{-}RS)_2(aq)$ complexes in *Geobacter sulfurreducens* incubation assays. While these species were predicted to be insignificant at equilibrium conditions of the bulk porewater in the wetlands included in the present study, such species might contribute to the bioavailable Hg^{II} pool locally under kinetically constrained conditions.

Another possibility is that the correlation between LMM–RSH compounds and Hg^{II} methylation potential observed in our and previous studies reflects mechanisms unrelated to the chemical speciation of $Hg^{II}(aq)$. Microorganisms produce certain LMM thiols (Kiene et al., 1990; Kiene and Taylor, 1988; Leclerc et al., 2015) and their concentration may thus be linked to microbial activity. Among the detected LMM thiol compounds, Cys, NACCys, HCys, Pen, GluCys and GSH are reported to be of direct biological origin (Hand and Honek, 2005; Meister and Anderson, 1983; Selhub, 1999; Winters et al., 1995) while MAC, Glyc, 2MPA, and SUC can be formed by both indirect and direct biological processes (Brandt et al., 2015; Kiene, 1991; Kiene et al., 1990; Kiene and Taylor, 1988). For each individual wetland, the

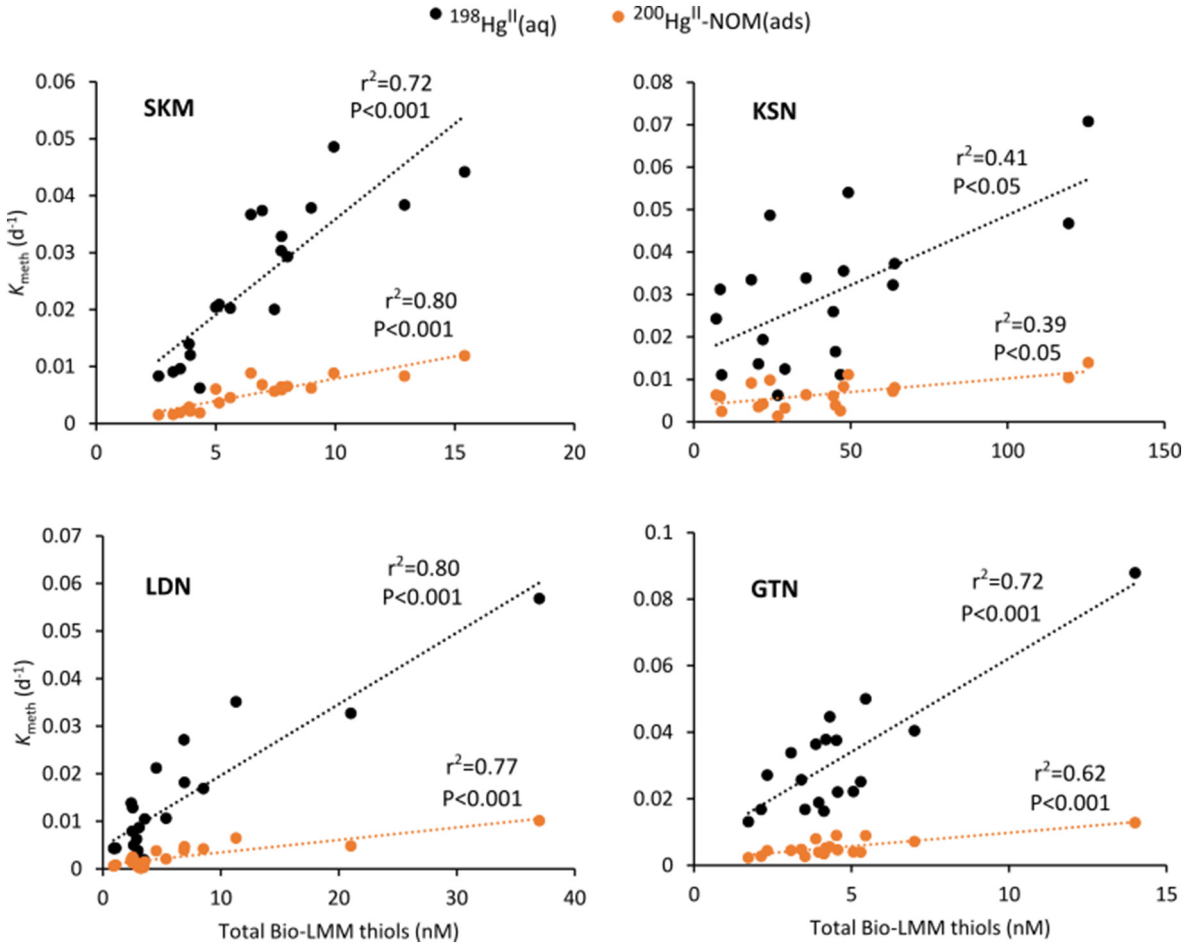

Fig. 3. Relationships between the concentration of total thiols (RSH + RSSR), summed for the subset of thiol compounds of direct biological origin, Total Bio-LMM thiols (Cys + NACCys+HCys+Pen+GluCys+GSH + Glyc), and the Hg^{II} methylation rate constant (k_{meth}) for the two tracers $^{198}Hg^{II}$(aq) and $^{200}Hg^{II}$-NOM(ads) at each of the four sampling sites.

correlation with k_{meth} (Fig. 3) was stronger with the RSH + RSSR forms of the subset of LMM thiols of direct biological origin (Cys+NACCys+HCys+Pen+GluCys+GSH), as compared to the correlation between k_{meth} and all the LMM thiol compounds (Fig. S4). In line with this result, Leclerc et al. (2015) found significant correlations between the biologically produced GSH related thiols GluCys, Cys and GSH and MeHg concentration in freshwater biofilms, but no correlation between MAC that is not of direct biological origin, and MeHg. In our study the "biological" thiols constituted on average 20–30% of the total concentration of LMM thiols at sites SKM, LDN and GTN, and 5% at KSN. The most abundant LMM thiol in this group was in most cases Cys (range 20–100%, average 70%), except at the KSN site. Since the thiols were present in dark, anaerobic soil porewaters, it is possible that they are produced by microbes under dark conditions rather than by photosynthetically active organisms. Bouchet et al. (2018) found higher concentrations of LMM–RSH compounds in periphyton and benthic biofilms under dark conditions compared to at sunlight exposure. Adediran et al. (2019) recently showed that under laboratory assay conditions *Geobacter sulfurreducens* can metabolically produce and export appreciable amounts of LMM–RSH compounds reaching concentrations up to 100 nM in the assay medium. At present, it is not known how widespread these processes are among microbial taxa or how prevalent they are in wetland soils. However, Xu (2018) identified *Geobacteraceae* as the predominant taxonomic family carrying the *hgcA* gene in the wetland soils in our study. Considering the studies by Adedrian et al. and Xu et al. our results may suggest that the correlation between RSH + RSSR forms of the "biological" LMM thiols and k_{meth} is reflecting a functional relationship between the activity of methylating microbes (and likely the total microbial activity) and k_{meth}.

3.5. Implications for microbial uptake of Hg^{II} in boreal wetland soils

Our study presents a comprehensive and detailed thermodynamic speciation model for Hg and includes Hg^{II}(aq) complexes with LMM–RSH compounds when linking Hg^{II} speciation to methylation in natural environments. Results showed that the time-dependent solubility and sorption/desorption of Hg^{II} is one primary controlling factor for MeHg formation in 48 h incubation experiments, and likely also under natural conditions in boreal wetlands. Further, this work corroborates previous findings (Bouchet et al., 2018; Leclerc et al., 2015), and is an advancement, by demonstrating significant correlations between the concentration of specific LMM–RSH compounds and k_{meth} in boreal wetland soils with large variations in biogeochemistry. This study showed that the correlation extends to lower concentrations of LMM–RSH compounds than what has been reported for biofilms. The mechanisms underlying this correlation are not yet fully understood, but the results in this work suggest that the correlation is not driven by the thermodynamic speciation of Hg^{II} in porewaters. As discussed above, the concentration of bulk $Hg(NOM\text{-}RS)_2(aq)$ complexes and of ternary Hg(LMM-RS)(NOM-RS)(aq) complexes were much higher than the concentrations of the specific $Hg(LMM\text{-}RS)_2(aq)$ complexes quantified in this study. Indeed, the specific LMM–RSH compounds which so far have been in focus in studies on Hg^{II} bioavailability and methylation constitute only a minor fraction of the total RSH pool in the wetland porewaters. Even

though the formation of $Hg(LMM\text{-}RS)_2(aq)$ complexes may still be important for MeHg formation, there is a need to further resolve the molecular structure and availability for microbial uptake and methylation of $Hg(NOM\text{-}RS)_2(aq)$ and $Hg(LMM\text{-}RS)(NOM\text{-}RS)(aq)$ complexes.

Author contribution

VL-N, US and EB designed the study, VL-N and EB carried out the field sampling, VL-N carried out all chemical analyses, VL-N, US and EB interpreted the data and VL-N, US and EB wrote the manuscript.

Declaration of competing interest

The authors declare that they have no known competing financial interests or personal relationships that could have appeared to influence the work reported in this paper.

Acknowledgements

This work was financially supported by the Swedish Research Council via the project Sino-Swedish Mercury Management Research Framework – SMaReF (2013-6978), the Kempe Foundations (SMK-2745, SMK-2840), the JC Kempe Memorial Scholarship Foundation, the Stiftelsen JC Kempes Minnes Stipendiefond, Umeå University and the Swedish University of Agricultural Sciences. Tomas Hedlund and Lars Lundmark are greatly acknowledged for technical support.

Appendix A. Supplementary data

Supplementary data to this article can be found online at https://doi.org/10.1016/j.scitotenv.2020.142666.

References

Adediran, G.A., Van, L.N., Song, Y., Schaefer, J.K., Skyllberg, U., Bjorn, E., 2019. Microbial biosynthesis of thiol compounds: implications for speciation, cellular uptake, and methylation of Hg(II). Environ. Sci. Technol. 53, 8187–8196.

Benoit, J.M., Gilmour, C.C., Mason, R.P., Heyes, A., 1999. Sulfide controls on mercury speciation and bioavailability to methylating bacteria in sediment pore waters. Environ. Sci. Technol. 33, 951–957.

Benoit, J.M., Gilmour, C.C., Mason, R.P., 2001a. Aspects of bioavailability of mercury for methylation in pure cultures of Desulfobulbus propionicus (1pr3). Appl. Environ. Microbiol. 67, 51–58.

Benoit, J.M., Gilmour, C.C., Mason, R.P., 2001b. The influence of sulfide on solid phase mercury bioavailability for methylation by pure cultures of Desulfobulbus propionicus (1pr3). Environ. Sci. Technol. 35, 127–132.

Benoit, J.M., Gilmour, C.C., Heyes, A., Mason, R.P., Miller, C.L., 2003. Geochemical and biological controls over methylmercury production and degradation in aquatic ecosystems. ASC Symposium Series 835, 262–297.

Bouchet, S., Goni-Urriza, M., Monperrus, M., Guyoneaud, R., Fernandez, P., Heredia, C., Tessier, E., Gassie, C., Point, D., Guedron, S., Acha, D., Amouroux, D., 2018. Linking microbial activities and low-molecular-weight thiols to hg methylation in biofilms and periphyton from high-altitude tropical lakes in the Bolivian Altiplano. Environ. Sci. Technol. 52, 9758–9767.

Brandt, U., Deters, A., Steinbuchel, A., 2015. A jack-of-all-trades: 2-mercaptosuccinic acid. Appl. Microbiol. Biotechnol. 99, 4545–4557.

Bravo, A.G., Bouchet, S., Tolu, J., Bjorn, E., Mateos-Rivera, A., Bertilsson, S., 2017. Molecular composition of organic matter controls methylmercury formation in boreal lakes. Nat. Commun. 8, 14255.

Burton, E.D., Bush, R.T., Johnston, S.G., Sullivan, L.A., Keene, A.F., 2011. Sulfur biogeochemical cycling and novel Fe-S mineralization pathways in a tidally re-flooded wetland. Geochim. Cosmochim. Acta 75, 3434–3451.

Chiasson-Gould, S.A., Blais, J.M., Poulain, A.J., 2014. Dissolved organic matter kinetically controls mercury bioavailability to bacteria. Environ. Sci. Technol. 48, 3153–3161.

Compeau, G.C., Bartha, R., 1985. Sulfate-reducing bacteria: principal methylators of mercury in anoxic estuarine sediment. Appl. Environ. Microbiol. 50, 498–502.

Drott, A., Lambertsson, L., Bjorn, E., Skyllberg, U., 2007. Importance of dissolved neutral mercury sulfides for methyl mercury production in contaminated sediments. Environ. Sci. Technol. 41, 2270–2276.

Drott, A., Bjorn, E., Bouchet, S., Skyllberg, U., 2013. Refining thermodynamic constants for mercury(II)-sulfides in equilibrium with Metacinnabar at sub-micromolar aqueous sulfide concentrations. Environ. Sci. Technol. 47, 4197–4203.

Dyrssen, D., Wedborg, M., 1991. The sulfur-mercury(II) system in natural waters. Water Air Soil Pollut. 56, 507–519.

Fleming, E.J., Mack, E.E., Green, P.G., Nelson, D.C., 2006. Mercury methylation from unexpected sources: molybdate-inhibited freshwater sediments and an iron-reducing bacterium. Appl. Environ. Microbiol. 72, 457–464.

Gilmour, C.C., Henry, E.A., Mitchell, R., 1992. Sulfate stimulations of mercury methylation in fresh-water sediments. Environ. Sci. Technol. 26, 2281–2287.

Gilmour, C.C., Podar, M., Bullock, A.L., Graham, A.M., Brown, S.D., Somenahally, A.C., Johs, A., Hurt, R.A., Bailey, K.L., Elias, D.A., 2013. Mercury methylation by novel microorganisms from new environments. Environ. Sci. Technol. 47, 11810–11820.

Hamelin, S., Amyot, M., Barkay, T., Wang, Y.P., Planas, D., 2011. Methanogens: principal methylators of mercury in Lake Periphyton. Environ. Sci. Technol. 45, 7693–7700.

Hand, C.E., Honek, J.F., 2005. Biological chemistry of naturally occurring thiols of microbial and marine origin. J. Nat. Prod. 68, 293–308.

Hollweg, T.A., Gilmour, C.C., Mason, R.P., 2010. Mercury and methylmercury cycling in sediments of the mid-Atlantic continental shelf and slope. Limnol. Oceanogr. 55, 2703–2722.

Jay, J.A., Morel, F.M.M., Hemond, H.F., 2000. Mercury speciation in the presence of polysulfides. Environ. Sci. Technol. 34, 2196–2200.

Jay, J.A., Murray, K.J., Gilmour, C.C., Mason, R.P., Morel, F.M.M., Roberts, A.L., Hemond, H.F., 2002. Mercury methylation by Desulfovibrio desulfuricans ND132 in the presence of polysulfides. Appl. Environ. Microbiol. 68, 5741–5745.

Jiskra, M., Saile, D., Wiederhold, J.G., Bourdon, B., Bjorn, E., Kretzschmar, R., 2014. Kinetics of Hg(II) exchange between organic ligands, goethite, and natural organic matter studied with an enriched stable isotope approach. Environ. Sci. Technol. 48, 13207–13217.

Jonsson, S., Skyllberg, U., Nilsson, M.B., Westlund, P.O., Shchukarev, A., Lundberg, E., Bjorn, E., 2012. Mercury methylation rates for geochemically relevant Hg-II species in sediments. Environ. Sci. Technol. 46, 11653–11659.

Jonsson, S., Skyllberg, U., Nilsson, M.B., Lundberg, E., Andersson, A., Björn, E., 2014. Differentiated availability of geochemical mercury pools controls methylmercury levels in estuarine sediment and biota. Nat. Commun. 5, 4624.

Kampalath, R.A., Lin, C.C., Jay, J.A., 2013. Influences of zero-valent sulfur on mercury methylation in bacterial cocultures. Water Air Soil Pollut. 224.

Karlsson, M., Lindgren, J., 2012. www.winsgw.se.

Kerin, E.J., Gilmour, C.C., Roden, E., Suzuki, M.T., Coates, J.D., Mason, R.P., 2006. Mercury methylation by dissimilatory iron-reducing bacteria. Appl. Environ. Microbiol. 72, 7919–7921.

Kiene, R.P., 1991. Evidence for the biological turnover of thiols in anoxic marine sediments. Biogeochemistry 13, 117–135.

Kiene, R.P., Taylor, B.F., 1988. Demethylation of dimethylsulfoniopropionate and production of thiols in anoxic marine sediments. Appl. Environ. Microbiol. 54, 2208–2212.

Kiene, R.P., Malloy, K.D., Taylor, B.F., 1990. Sulfur-containing amino-acids as precursors of thiols in anoxic coastal sediments. Appl. Environ. Microbiol. 56, 156–161.

Kim, M., Han, S., Gieskes, J., Deheyn, D.D., 2011. Importance of organic matter lability for monomethylmercury production in sulfate-rich marine sediments. Sci. Total Environ. 409, 778–784.

Lambertsson, L., Bjorn, E., 2004. Validation of a simplified field-adapted procedure for routine determinations of methyl mercury at trace levels in natural water samples using species-specific isotope dilution mass spectrometry. Anal. Bioanal. Chem. 380, 871–875.

Lambertsson, L., Lundberg, E., Nilsson, M., Frech, W., 2001. Applications of enriched stable isotope tracers in combination with isotope dilution GC-ICP-MS to study mercury species transformation in sea sediments during in situ ethylation and determination. J. Anal. At. Spectrom. 16, 1296–1301.

Leclerc, M., Planas, D., Amyot, M., 2015. Relationship between extracellular low-molecular-weight thiols and mercury species in natural lake periphytic biofilms. Environ. Sci. Technol. 49, 7709–7716.

Liem-Nguyen, V., Bouchet, S., Bjorn, E., 2015. Determination of sub-nanomolar levels of low molecular mass thiols in natural waters by liquid chromatography tandem mass spectrometry after derivatization with p-(Hydroxymercuri)benzoate and online preconcentration. Anal. Chem. 87, 1089–1096.

Liem-Nguyen, V., Jonsson, S., Skyllberg, U., Nilsson, M.B., Andersson, A., Lundberg, E., Bjorn, E., 2016. Effects of nutrient loading and mercury chemical speciation on the formation and degradation of methylmercury in estuarine sediment. Environ. Sci. Technol. 50, 6983–6990.

Liem-Nguyen, V., Skyllberg, U., Bjorn, E., 2017a. Thermodynamic modeling of the solubility and chemical speciation of mercury and methylmercury driven by organic thiols and micromolar sulfide concentrations in boreal wetland soils. Environ. Sci. Technol. 51, 3678–3686.

Liem-Nguyen, V., Skyllberg, U., Nam, K., Bjorn, E., 2017b. Thermodynamic stability of mercury(II) complexes formed with environmentally relevant low-molecular-mass thiols studied by competing ligand exchange and density functional theory. Environ. Chem. 14, 243–253.

Meister, A., Anderson, M.E., 1983. Glutathione. Annu. Rev. Biochem 52, 711–760.

Mergler, D., Anderson, H.A., Chan, L.H.M., Mahaffey, K.R., Murray, M., Sakamoto, M., Stern, A.H., 2007. Methylmercury exposure and health effects in humans: a worldwide concern. Ambio 36, 3–11.

Millero, F.J., 1986. The thermodynamics and kinetics of the hydrogen sulfide system in natural waters. Mar. Chem. 18, 121–147.

Olsen, T.A., Muller, K.A., Painter, S.L., Brooks, S.C., 2018. Kinetics of methylmercury production revisited. Environ. Sci. Technol. 52, 2063–2070.

Parks, J.M., Johs, A., Podar, M., Bridou, R., Hurt, R.A., Smith, S.D., Tomanicek, S.J., Qian, Y., Brown, S.D., Brandt, C.C., Palumbo, A.V., Smith, J.C., Wall, J.D., Elias, D.A., Liang, L.Y., 2013. The genetic basis for bacterial mercury methylation. Science 339, 1332–1335.

Pei, K.L., Sooriyaarachchi, M., Sherrell, D.A., George, G.N., Gailer, J., 2011. Probing the coordination behavior of Hg2+, CH3Hg+, and Cd2+ towards mixtures of two biological thiols by HPLC-ICP-AES. J. Inorg. Biochem. 105, 375–381.

Qian, J., Skyllberg, U., Frech, W., Bleam, W.F., Bloom, P.R., Petit, P.E., 2002. Bonding of methyl mercury to reduced sulfur groups in soil and stream organic matter as determined by X-ray absorption spectroscopy and binding affinity studies. Geochim. Cosmochim. Acta 66, 3873–3885.

Rabenstein, D.L., Isab, A.A., 1982. A proton nuclear magnetic-resonance study of the interaction of mercury with intact human-erythrocytes. Biochim. Biophys. Acta 721, 374–384.

Schaefer, J.K., Morel, F.M.M., 2009. High methylation rates of mercury bound to cysteine by Geobacter sulfurreducens. Nat. Geosci. 2, 123–126.

Schaefer, J.K., Rocks, S.S., Zheng, W., Liang, L.Y., Gu, B.H., Morel, F.M.M., 2011. Active transport, substrate specificity, and methylation of Hg(II) in anaerobic bacteria. Proc. Natl. Acad. Sci. U. S. A. 108, 8714–8719.

Scheulhammer, A.M., Meyer, M.W., Sandheinrich, M.B., Murray, M.W., 2007. Effects of environmental methylmercury on the health of wild birds, mammals, and fish. Ambio 36, 12–18.

Schwartz, G.E., Olsen, T.A., Muller, K.A., Brooks, S.C., 2019. Ecosystem controls on methylmercury production by periphyton biofilms in a contaminated stream: implications for predictive modeling. Environ. Toxicol. Chem. 38, 2426–2435.

Schwarzenbach, G.W.M., 1963. Die Loslichkeit Von Metallsulfiden.1. Schwarzes Quecksilbersulfid. Helv. Chim. Acta 46, 2613–2628.

Selhub, J., 1999. Homocysteine metabolism. Annu. Rev. Nutr. 19, 217–246.

Skyllberg, U., 2008. Competition among thiols and inorganic sulfides and polysulfides for Hg and MeHg in wetland soils and sediments under suboxic conditions: illumination of controversies and implications for MeHg net production. J. Geophys. Res-Biogeo. 113.

Skyllberg, U., Drott, A., 2010. Competition between disordered Iron sulfide and natural organic matter associated thiols for mercury(II)-an EXAFS study. Environ. Sci. Technol. 44, 1254–1259.

Skyllberg, U., Bloom, P.R., Qian, J., Lin, C.M., Bleam, W.F., 2006. Complexation of mercury (II) in soil organic matter: EXAFS evidence for linear two-coordination with reduced sulfur groups. Environ. Sci. Technol. 40, 4174–4180.

Song, Y., Jiang, T., Liem-Nguyen, V., Sparrman, T., Björn, E., Skyllberg, U., 2018. Thermodynamics of Hg(II) bonding to thiol groups in Suwannee River natural organic matter resolved by competitive ligand exchange, Hg LIII-edge EXAFS and 1H NMR spectroscopy. Environ. Sci. Technol. 52, 8292–8301.

Tjerngren, I., Karlsson, T., Bjorn, E., Skyllberg, U., 2012a. Potential Hg methylation and MeHg demethylation rates related to the nutrient status of different boreal wetlands. Biogeochemistry 108, 335–350.

Tjerngren, I., Meili, M., Bjorn, E., Skyllberg, U., 2012b. Eight boreal wetlands as sources and sinks for methyl mercury in relation to soil acidity, C/N ratio, and small-scale flooding. Environ. Sci. Technol. 46, 8052–8060.

USEPA, 2002. Method 1631, Revision E: Mercury in Water by Oxidation, Purge and Trap, and Cold Vapor Atomic Fluorescence Spectrometry (Washington, DC).

Winters, R.A., Zukowski, J., Ercal, N., Matthews, R.H., Spitz, D.R., 1995. Analysis of glutathione, glutathione disulfide, cysteine, homocysteine, and other biological thiols by high-performance liquid chromatography following derivatization by N-(1-pyrenyl) maleimide. Anal. Biochem. 227, 14–21.

Xu, J., 2018. Remediation of mercury contaminated soil and biological mercury methylation in the landscape. PhD Thesis. Department of Ecology and Genetics, Limnology. Uppsala University, Uppsala, Sweden.

Zhu, W., Song, Y., Adediran, G.A., Jiang, T., Reis, A.T., Pereira, E., Skyllberg, U., Bjorn, E., 2018. Mercury transformations in resuspended contaminated sediment controlled by redox conditions, chemical speciation and sources of organic matter. Geochim. Cosmochim. Acta 220, 158–179.